Title

A Noncanonical Role for the CKI-RB-E2F Cell-Cycle Signaling Pathway in Plant Effector-Triggered Immunity

Journal

Cell Host & Microbe, 16(6)

ISSN

1931-3128

Authors

Wang, Shui
Gu, Yangnan
Zebell, Sophia G
et al.

Publication Date

2014-12-01

DOI

10.1016/j.chom.2014.10.005

Peer reviewed

Published in final edited form as:
Cell Host Microbe. 2014 December 10; 16(6): 787–794. doi:10.1016/j.chom.2014.10.005.

A Noncanonical Role for the CKI-RB-E2F Cell Cycle Signaling Pathway in Plant Effector-Triggered Immunity

Shui Wang[1,2,*], **Yangnan Gu**[2,*], **Sophia G. Zebell**[2,*], **Lisa K. Anderson**[2], **Wei Wang**[2], **Rajinikanth Mohan**[2], and **Xinnian Dong**[2]

[1]Shanghai Center for Plant Stress Biology, Shanghai Institutes for Biological Sciences, Chinese Academy of Sciences, Shanghai 201602, China

[2]Howard Hughes Medical Institute-Gordon and Betty Moore Foundation, Department of Biology, PO Box 90338, Duke University, Durham, North Carolina 27708, USA

SUMMARY

Effector-triggered immunity (ETI), the major host defense mechanism in plants, is often associated with programmed cell death (PCD). Plants lack close homologs of caspases, the key mediators of PCD in animals. So although the NB-LRR receptors involved in ETI are well studied, how they activate PCD and confer disease resistance remains elusive. We show that the *Arabidopsis* nuclear envelope protein, CPR5, negatively regulates ETI and the associated PCD through a physical interaction with CYCLIN-DEPENDENT KINASE INHIBITORs (CKIs). Upon ETI induction, CKIs are released from CPR5 to cause over-activation of another core cell cycle regulator, E2F. In *cki* and *e2f* mutants, ETI responses induced by both TIR-NB-LRR and CC-NB-LRR classes of immune receptors are compromised. We further show that E2F is deregulated during ETI probably through CKI-mediated hyperphosphorylation of RETINOBLASTOMA-RELATED 1 (RBR1). This study demonstrates that canonical cell cycle regulators also play important noncanonical roles in plant immunity.

Correspondence: Shui Wang (swang@sibs.ac.cn), Xinnian Dong (xdong@duke.edu).
*These authors contributed equally to this work.

AUTHOR CONTRIBUTIONS

SW, YG, SGZ, LKA, WW and RM designed and performed the experiments, XD supervised the project. All authors participated in the manuscript preparation.

ACCESSION NUMBERS

The Gene Expression Omnibus accession numbers for the microarray data reported in this paper are GSE40322, GSE34047 (Pajerowska-Mukhtar et al., 2012), GSE58954, and GSE5745 (Anderson, 2006).

SUPPLEMENTAL INFORMATION

Supplemental Information includes four figures, four tables, Supplemental Experimental Procedures and References.

INTRODUCTION

Each plant genome encodes hundreds of NUCLEOTIDE-BINDING LEUCINE-RICH REPEAT (NB-LRR) proteins, which are structurally similar to the mammalian intracellular innate immune receptors, NOD-LIKE RECEPTORs (NLRs) (Ausubel, 2005). In the mammalian system, activation of NLRs can trigger programmed cell death (PCD) through recruitment of caspases (Ting et al., 2008). In plants, the presence of a pathogen effector detected by the cognate NB-LRR triggers ETI accompanied with rapid and often visible PCD (Jones and Dangl, 2006). However, plant genomes do not carry close homologs of caspases, but more distant metacaspases (Coll et al., 2010). Therefore, PCD is likely executed in plants through a unique mechanism.

In mammals, expression of caspases is tightly controlled by two transcription factors (TFs): p53 and E2F (Polager and Ginsberg, 2009). Although a homolog of the p53 protein has not been found in plants, all of the core E2F signaling proteins, including CDK INHIBITORS (CKIs), CYCLIN-DEPENDENT KINASES (CDKs), RETINOBLASTOMA (RB) and E2Fs, are present and function as their mammalian counterparts (De Veylder et al., 2007), but their roles in regulating plant immunity are not known.

Genetic screens performed in *Arabidopsis* have identified ENHANCED DISEASE SUSCEPTIBILITY 1 (EDS1) as a key downstream signaling component for the Toll Interleukin 1 Receptor (TIR)-NB-LRR class of immune receptors (Parker et al., 1996). To confer full immunity, the nucleocytoplasmic coordination of the effector/NB-LRR/EDS1 protein complex is required (Bhattacharjee et al., 2011; Heidrich et al., 2011). This requirement was also implicated genetically through isolation of the *modifier of snc1* (*mos*) mutants. Mutations in the nuclear transport receptor (*mos6*) and nuclear pore complex (*mos3* and *mos7*) blocked nuclear retention of some NB-LRRs as well as EDS1 and compromised resistance (Cheng et al., 2009). These data suggest that the nuclear membrane is a potential regulatory site of plant immune signaling.

Besides EDS1 and MOSs, which are positive regulators of NB-LRR-mediated immunity, “lesion mimic” mutants have also been studied extensively in searches for negative regulators of effector-triggered PCD and resistance. The *lesion simulating disease 1* (*lsd1*) mutant was found to have runaway PCD upon pathogen challenge due to improper activation of a class of “helper” NB-LRR proteins which act downstream of effector-specific NB-LRRs (Bonardi et al., 2011). Recently, a cell death enhancer mutant screen discovered that misregulation of the ANAPHASE-PROMOTING COMPLEX/CYCLOSOME (APC/C), a ubiquitin E3 ligase complex controlling cell cycle progression, could lead to upregulation of *NB-LRR* gene expression (Bao et al., 2013). Since these negative regulators function upstream of EDS1 (Bao et al., 2013; Rusterucci et al., 2001), the signaling components linking EDS1 to activation of PCD genes remain to be discovered.

The *Arabidopsis* lesion-mimic mutant *constitutive expresser of pathogenesis-related genes 5* (*cpr5*) may shed light on this downstream signaling pathway. The *cpr5* mutant has enhanced resistance to biotrophic pathogens *Pseudomonas syringae* pv. *maculicola* (*Psm*) and *Hyaloperonospora arabidopsidis* (*Hpa*) (Bowling et al., 1997; Kirik et al., 2001). However,

unlike the other lesion mimic mutants, the *cpr5* phenotype could not be suppressed by *eds1* (Clarke et al., 2001), suggesting that the mutation affects a component either downstream of EDS1 or independent of it (Figure S1A). Nor was the phenotype of *cpr5* significantly affected by *non-expresser of pathogenesis-related genes 1* (*npr1*), a mutant insensitive to the immune signal salicylic acid (SA) (Clarke et al., 2000). However, blocking SA accumulation with the *eds5* mutant did suppress the disease resistance phenotype of *cpr5*, but not its lesioning phenotype nor the stunted growth morphology, placing *cpr5* upstream of SA synthesis (Figure S1A). These results are consistent with the fact that SA, which is often produced during ETI (Vlot et al., 2009), is not only an essential signal in conferring NPR1-dependent resistance, but is also involved in augmenting ETI in an NPR1-independent manner (Feys et al., 2001). Apparently, in the *cpr5* mutant, this NPR1-independent defense is sufficiently activated to confer disease resistance.

In this study, we show that mutations of two *CKI*s, *SIAMESE* (*SIM*) and *SIAMESE-RELATED 1* (*SMR1*), fully suppressed pleiotropic phenotypes of *cpr5*. CPR5 is localized to the nuclear envelope where it physically interacts with SIM and this interaction is dynamically regulated during ETI. In both the *cpr5* mutant and wild-type (WT) plants undergoing ETI, SIM and SMR1 are involved in hyperphosphorylation of the cell cycle regulator RETINOBLASTOMA RELATED 1 (RBR1) and overexpression of E2F target genes. In addition, both the *sim smr1* and the *e2f* mutants are compromised in resistance. Our study, therefore, reveals a cell cycle-related signaling pathway for ETI.

RESULTS

CPR5 Is a Negative Regulator of Plant PCD and ETI

CPR5 was first discovered in a genetic screen for mutants with spontaneous PCD and constitutively enhanced resistance to biotrophic pathogens (Bowling et al., 1997). The CPR5 protein has 4–5 predicted transmembrane domains (TMs) (Figure S1B) and was detected predominantly in the nuclear membrane but not the plasma membrane fraction (Figures S1C and S1D). To address whether CPR5 plays a direct role in defense, we analyzed independent *35S:GFP-CPR5 Arabidopsis* transgenic lines in the *cpr5* mutant background. We found that transgenic lines with different levels of the GFP-CPR5 protein (Figure 1A) could fully complement the *cpr5* mutant morphology, similar to those with the transgene driven by the native *CPR5* promoter (Figure S1E). In contrast to the loss-of-function *cpr5* mutant, these transgenic lines showed compromised PCD and diminished immunity against the bacterial pathogen *Psm* ES4326/*AvrRpt2* (Figures 1B and 1C). These data demonstrate that CPR5 is a negative regulator of PCD and immunity against biotrophic pathogens.

CPR5 Negatively Regulates ETI through Association with the KRP Family of CKIs

To further understand CPR5 function, we carried out a genetic screen for suppressors of *cpr5* in NPR1-independent *Hpa* resistance (*svi* mutants; Figures 1D and S1F). The recessive *svi1* mutation was mapped to a deletion containing 6 putative genes (Figure S1G and Table S1). Among them, *KIP-RELATED PROTEIN 2* (*KRP2*) belongs to the KRP family of CKIs. Both KRP2 and a close member of this family, KRP1, have been found previously to control cell cycle progression, cell death and trichome development (Schnittger et al., 2003; Verkest

et al., 2005), which is relevant to the phenotype of *cpr5*. Similar to *svi1*, a *krp2* T-DNA insertion mutation also partially restored *Hpa* Noco2 susceptibility when crossed into the *cpr5 npr1* mutant and *krp2* and *npr1* have additive effects on suppression of *cpr5*-induced resistance (Figure 1E).

The KRP family contains at least 18 members and is homologous to the human Cip/Kip (CDK interacting protein/Kinase inhibitory protein) proteins (Figure S1H and Table S2) (Wang et al., 1997). To determine the functional redundancy of *Arabidopsis KRP* genes in resistance observed in c*pr5*, we crossed *cpr5* with other *krp* mutants. While the *krp1 krp2* double mutant was not viable, the *siamese* (*sim*) *siamese-related 1* (*smr1*) double mutant dramatically suppressed *cpr5* morphological phenotypes (data not shown) and resistance (Figure 1F). Therefore, SIM and SMR1 function redundantly downstream of CPR5 and play a positive role in defense against *Hpa*.

To determine the relationship between CPR5 and SIM/SMR1, we first ruled out a possible regulation at the transcriptional or the translational level (Figures S1I and S1J). We then tested whether CPR5 and SIM/SMR1 function in the same protein complex. Bimolecular Fluorescence Complementation (BiFC) showed that they could interact *in vivo* in the nuclear periphery (Figures 1G and S1K). This interaction was further verified by a split luciferase assay (Figures 1H and S1L) and yeast two-hybrid analysis (Figure S1M). These results demonstrate that CPR5 not only genetically but also physically interacts with CKIs.

To reveal the regulatory mechanism of this interaction, we performed a semi-*in vitro* co-immunoprecipitation experiment by adding recombinant SIM protein to extracts prepared from leaves infected with either *Psm* ES4326 or *Psm* ES4326/*AvrRpt2*. While no degradation of the recombinant SIM protein was detected, we found that its association with CPR5 was reduced in response to *Psm* ES4326/*AvrRpt2*, but not to *Psm* ES4326 (Figure 1I). This result suggests that CPR5 may negatively regulate SIM through the physical interaction, which can be disrupted upon ETI induction. However, detailed molecular mechanism and the kinetics of the interaction at the physiological level require further investigation.

CPR5 Regulates ETI-Specific Defense Gene Expression through SIM/SMR1 and E2F

The epistatic relationship of *sim smr1* to *cpr5* was further confirmed by the whole genome microarray analysis (GEO#: GSE40322). As shown in Figure 2A, WT, *sim smr1* and *cpr5 sim smr1* shared expression patterns at the whole genome level, which were largely distinct from that of the *cpr5* mutant. Volcano plots of differentially expressed genes in *cpr5* and *cpr5 sim smr1* also revealed an overwhelming dependency of the *cpr5*-induced transcriptomic changes on SIM/SMR1 (Figure 2B). To further quantify this dependency, we built a series of statistical models and performed factorial analysis. As shown in Figure S2A, in all cases, ~90% of *cpr5*-upregulated genes were dependent on SIM/SMR1, further confirming that SIM and SMR1 are required for *cpr5*-mediated gene expression.

Further characterization of *cpr5*-mediated differentially expressed genes (*t*-test, p-value < 0.05, FC > 2) (Figures 2C, S2B, and Table S3) revealed that the most significantly enriched gene ontology term (http://www.geneontology.org/) was “defense-related” (hypergeometric

test, *p*-value 0). Comparative analysis with three other defense-related microarray data sets (GSE34047, GSE58954) revealed significant overlap with *Psm* ES4326/*AvrRpt2*-induced genes and the SA-induced genes, but limited overlap with the microbe-associated molecular pattern (MAMP) elf18-induced genes (Figures 2D and S2C). Since the SA signaling mutant *npr1* had little effect on *cpr5* at the genomic level (GSE5745, Figure S2D), we concluded that the *cpr5* mutation could induce defense genes independent of NPR1, consistent with the genetic data (Clarke et al., 2000) (Figure S1A).

The microarray data clearly support our hypothesis that CPR5 and SIM/SMR1 are negative and positive regulators of ETI, respectively. Since SA is produced during ETI, it is not surprising that there was a significant overlap between *Psm* ES4326/*AvrRpt2*- and SA-induced genes, which comprised the majority of *cpr5*-induced genes (Figures 2D and S2C). Moreover, in *cpr5 sim smr1*, both the SA synthesis gene expression and the SA level were restored to WT (Figures S2E and S2F).

To understand how SIM/SMR1 positively controls defense gene expression, we considered the canonical core cell cycle signaling pathway CKI-CDK-RB-E2F (Sherr and Roberts, 1999) because the CKI function of SIM/SMR1 has been previously demonstrated (Walker et al., 2000). We found that among the top 20 induced genes in *cpr5* (based on *p*-values), 9 are also significantly induced in E2Fa/DPa-overexpressing transgenic plants (Vandepoele et al., 2005) (Figure 2E). E2Fs are known downstream TFs of cell cycle, cell death and immune response in mammals (Polager and Ginsberg, 2008). To study the role of *E2F* genes in plants, we first examined the mutants of all three canonical *E2F* genes of *Arabidopsis*. We found that the double mutants were indistinguishable from WT in plant growth (data not shown) while the *e2fa e2fb e2fc* triple mutant (*e2fabc*) showed near normal vegetative growth, but severely compromised fertility (Figure S2G). This result indicates that these three E2Fs play a redundant role in *Arabidopsis* reproduction. We found that in the *cpr5 e2fabc* quadruple mutant, defense genes up-regulated in *cpr5* were fully restored to WT levels (Figure 2F). Moreover, similar to *sim smr1*, *e2fabc* was more susceptible to *Psm* ES4326 than WT (Figure S2H). These data suggest that CPR5 and SIM/SMR1 may signal through E2F during the plant immune response.

SIM/SMR1 and E2F Are Required for Pathogen Effector-Triggered PCD and Immunity

Our microarray data suggest that like mammalian Cip/Kip proteins, which are known to play a key role in integrating stress signals into cell fate determination (Besson et al., 2008), plant CKIs and E2Fs may be important regulators of PCD in response to pathogen challenge. This is consistent with the genetic data showing that the *cpr5*-associated PCD in cotyledons was fully suppressed by both *sim smr1* and *e2fabc* (Figures 3A and 3B). To further test whether the CPR5-SIM/SMR-E2F signaling pathway plays a role in ETI, we inoculated *sim smr1* and *e2fabc* with *Psm* ES4326/*AvrRpt2*. After 24 hours, a strong effector-triggered PCD and resistance were observed in WT plants, but not in *sim smr1* and *e2fabc*, similar to the *resistant to pseudomonas syringae 2* (*rps2*) mutant lacking the cognate coiled coil (CC)-NB-LRR immune receptor for AvrRpt2 (Figures 3C, 3D and S3A). This indicates that SIM/SMR1 and E2Fs are downstream components required for the onset of ETI. The defense phenotype of the mutants was unlikely to be due to a deficiency in SA synthesis, which was

only slightly delayed in the *sim smr1* mutant after *Psm* ES4326/*AvrRpt2* inoculation (Figure S3B). We also performed an infection experiment using *Hpa* Emwa1 for which the *Arabidopsis* Col-0 accession carries the TIR-NB-LRR class of immune receptor, RPP4. We found that similar to the *RPP4*-deficient Ws accession, *sim smr1* and *e2fabc* were compromised in RPP4-mediated ETI (Figure 3E), indicating that SIM/SMR1 and E2Fs are positive regulators of ETI mediated by both CC-NB-LRR (e.g., RPS2) and TIR-NB-LRR (e.g., RPP4) classes of immune receptors.

Even though the *sim smr1* and *e2fabc* mutants were also defective in basal resistance (Figure S2H), this phenotype was not discernible at the higher inoculum of *Psm* ES4326 without the effector (left panel, Figure 3D). Since *sim smr1* and *e2fabc* responded normally to MAMPs flg22 and elf18 (Figure S3C), their enhanced disease susceptibility may be caused by a deficiency downstream of the MAMP-triggered defense. Whether it involves a deficiency in the synthesis of SA, an inducer of general disease resistance in plants (Durrant and Dong, 2004), or compromised ETI triggered by other minor effectors in the pathogens remains to be tested.

CPR5 and SIM/SMR1 Control Effector-Triggered Immunity through Hyperphosphorylation of RBR1 and Activation of E2F

We next investigated how SIM and SMR1 control ETI. In mammals, the transcriptional activity of E2F is regulated by CKIs through CDK phosphorylation of RB. RB is normally bound to E2F to repress E2F activity. Phosphorylation of RB by CDK results in E2F release to activate G1 to S cell cycle transition. However, hyperphosphorylation of RB can instead lead to PCD (Harbour and Dean, 2000). To test the possibility that SIM and SMR1 regulate E2F activity through CDK-mediated phosphorylation of RBR1 in *Arabidopsis*, we first examined the level of CDKA1, a homolog of mammalian CDK2 which is a known regulator of RB (Harbour and Dean, 2000). We found that while the *CDKA1* transcript level was unaffected in *cpr5* (Figure S4A), more CDKA1 protein was detected in *cpr5* than WT, but not in *cpr5 sim smr1* (Figure S4B). This result indicates that in the absence of CPR5, SIM and SMR1 promote the accumulation of CDKA1. Overexpression of KRP2 had a similar effect on the CDKA1 protein (De Veylder et al., 2001), suggesting that these CKIs can not only inhibit the CDK activity but also stabilize the CDK protein.

The CDK target sequence in RB is highly conserved in both animals and plants (Figures S4C), allowing the antibody raised against the phosphorylated serine 807 (S807) of the human RB protein (α-P-RB) to recognize the phosphorylated serine 911 (S911) of the *Arabidopsis* RBR1 (Magyar et al., 2012). We further confirmed the specificity of this antibody (Figure S4D).

Using α-P-RB, we next examined RBR1 phosphorylation in the *cpr5* and *sim smr1* mutants. As shown in Figure 4A, RBR1 phosphorylation was increased in *sim smr1*, consistent with their role as CKIs. Intriguingly, in *cpr5*, RBR1 phosphorylation was also increased, consistent with the higher CDKA1 protein level detected in this mutant (Figure S4B). Moreover, an additional protein band was detected in *cpr5*. Since this upshifted band disappeared after CIP treatment, we postulated that it was RBR1 hyperphosphorylated at the additional CDK target sites (Figure S4E). More importantly, this additional band was

diminished in *cpr5 sim smr1* (Figure 4A), indicating that in *cpr5*, SIM and SMR1 acquired a novel activity of facilitating RBR1 hyperphosphorylation, possibly through CDKA1.

Based on these data, we hypothesize that RBR1 hyperphosphorylation (Figure 4A) and aberrant elevation of E2F activities (Figures 2E and 3) result in spontaneous PCD in *cpr5*. To investigate whether RBR1 hyperphosphorylation is a physiological response in ETI, we performed a western blot on plants infected with *Hpa* Emwa1. As shown in Figure 4B, the upshifted RBR1 band was also observed using α-P-RB one day after inoculation when effector-triggered PCD was expected to occur (Wang et al., 2011) and this band was significantly weakened in *rpp4*, a mutant of the cognate NB-LRR. We then tested RBR1 phosphorylation in ETI mediated by RPS2 and found that while RBR1 phosphorylation and hyperphosphorylation were induced after virulent *Psm* ES4326 infection, RBR1 hyperphosphorylation was markedly enhanced in WT plants inoculated with *Psm* ES4326/*AvrRpt2*, where effector-triggered PCD occurred (Figure 4C). This RBR1 hyperphosphorylation was blocked in *rps2*. In support of our hypothesis, the AvrRpt2-induced RBR1 hyperphosphorylation was also absent in *sim smr1* (right panel, Figure 4C). These data demonstrate that recognition of pathogen effectors by both the TIR-NB-LRR (e.g., RPP4) and CC-NB-LRR (e.g., RPS2) classes of immune receptors can trigger plant cell death and immunity through SIM/SMR1-mediated RBR1 hyperphosphorylation and subsequent over-activation of E2Fs.

DISCUSSION

The fundamental mechanism of cell cycle regulation is highly conserved among eukaryotes (Harashima et al., 2013). SIM and SMR1 are the plant counterparts of the mammalian Cip/Kip family of CKIs (Walker et al., 2000). These CKIs are known to control RB phosphorylation by inhibiting CDK activity. Our study shows that besides their canonical CKI function in cell cycle regulation, SIM and SMR1 acquire a new function of facilitating RBR1 hyperphosphorylation upon pathogen challenge (Figure 4D). Whether this is achieved through stabilization of CDKA1 (Figure S4B) or activation of a different kinase requires further investigation. This latter scenario is quite plausible given the fact that CKIs have flexible structures allowing them to bind different partners besides CDKs (Starostina and Kipreos, 2012).

Strikingly, activation of both TIR- and CC-NB-LRR NLR proteins induce hyperphosphorylation of RBR1 (Figures 4B and 4C) suggesting a general role for this regulatory mechanism in ETI. RBR1 hyperphosphorylation is correlated with the deregulation of E2F target genes (Figures 2E and 2F), which we propose leads to PCD and pathogen resistance (Figure 3). Like their counterparts in mammals (Polager and Ginsberg, 2009), the plant E2Fs can induce opposing biological processes, i.e., cell proliferation during normal development and PCD during ETI. For the immune response, higher levels of free E2F may be required as well as additional TFs, such as WRKYs, which can be specifically induced or activated upon pathogen challenge.

The *sim smr1* and *e2fabc* mutants are not only defective in ETI (Figure 3), but also more susceptible to virulent pathogens (Figures 1F and S2H). The underlying mechanism is not

clear since basal resistance could be conferred by different immune mechanisms and the interplay between them is complex and not completely understood. In a recent report, an atypical E2F, DEL1, was found to be a transcriptional repressor of SA biosynthesis (Chandran et al., 2014). Since the *sim smr1* and *e2fabc* mutants could only block SA biosynthesis induced in *cpr5* (Figure S2F), not by *Psm* ES4326/*AvrRpt2* (Figure S3B for *sim smr1*), a defect in SA synthesis is unlikely the explanation for the enhanced disease susceptibility in the mutants. Thus, the CPR5-CKI-RBR1-E2F signaling pathway is directly involved in ETI and affects basal resistance through an unknown mechanism.

EXPERIMENTAL PROCEDURES

Pathogen Infection

Infection of *Arabidopsis* plants with *Hpa* Noco2, *Hpa* Emwa1, and *Psm* ES4326 with or without AvrRpt2 was carried out as previously described (Fu et al., 2012; Wang et al., 2011).

Ion leakage Measurement

Psm ES4326/*AvrRpt2*-induced ion leakage was measured as previously described (Mackey et al., 2002).

Mutant Screen and Tiling Array-Based Cloning

The *cpr5-1 npr1-1* seeds were mutagenized using fast neutron bombardment. The genetic screen for *svi* mutants was carried out as described (Parker et al., 1996). Tiling array-based cloning was performed as described (Wang et al., 2010).

BiFC and Split Luciferase Assays

The split luciferase assay was carried out as described (Chen et al., 2008). The BiFC using the yellow fluorescence protein (YFP) was performed as described (Qi et al., 2012).

Co-Immunoprecipitation (co-IP)

Four-week-old plants were infiltrated with pathogen. Total Protein was extracted from 250mg of the infiltrated leaves in 1 ml IP buffer consisting 50 mM Tris (pH = 7), 150 mM NaCl, 0.1% Triton X-100, 0.2% NP-40, 40 μM MG115 and protease inhibitor (Sigma). HA-SIM protein (~0.5 μg) (synthesized by wheat germ-based TnT system, BioSieg, Tokushima, Japan) was added to plant extract and incubated with GFP-Trap agarose beads (ChromoTek, Martinsried, Germany) for indicated hours at 4°C. While 40 μl IP reaction was taken for SIM protein input control, beads in the remaining reaction were washed four times with IP buffer and then mixed with protein loading buffer containing 50 mM DTT.

Microarray Procedure and Analysis

The GeneChip *Arabidopsis* ATH1 Genome Arrays (Affymetrix, Santa Clara, CA) were processed as described (Pajerowska-Mukhtar et al., 2012; Wang et al., 2010). For the *cpr5*, *sim smr1* and *cpr5 sim smr1*dataset, 10-day-old seedlings were used for RNA preparation. For the ETI dataset, four-week-old plants were infected with *Psm* ES4326 carrying AvrRpt2

at OD_{600} 0.01 for 0 and 6 hours. The SA and elf18 datasets were published (Pajerowska-Mukhtar et al., 2012). Array data were summarized using the Robust Multi-array Average (RMA) method with the baseline transformed to the median of all samples. Statistical analysis was performed using GeneSpring (Agilent) and R packages.

Statistics

Unless otherwise stated, statistical analysis was performed by one-way analysis of variance (ANOVA) with Bonferroni post hoc test. The letter above the bar indicates a statistically significant difference between groups at p-value < 0.01.

Supplementary Material

Refer to Web version on PubMed Central for supplementary material.

Acknowledgments

We thank L. De Veylder for providing *e2fa-2 e2fb-1*, J. Wang for helping with the split luciferase assay. This work was supported by grants from NSF (IOS-0744602, MCB-0519898), NIH (2R01-GM069594-09) and by the HHMI-GBMF (through Grant GBMF3032) to X. Dong, a grant from Chinese Academy of Sciences (XDB11030700) to S. Wang, and a STAR graduate fellowship from the EPA to L. K. Anderson (EPA grant number U915894).

References

Anderson, LK. Biology. Duke University; 2006. CPR5 encodes a novel protein required for endoreduplication and cell expansion in plants; p. xviiip. 149

Ausubel FM. Are innate immune signaling pathways in plants and animals conserved? Nat Immunol. 2005; 6:973–979. [PubMed: 16177805]

Bao ZL, Yang HJ, Hua J. Perturbation of cell cycle regulation triggers plant immune response via activation of disease resistance genes. Proc Natl Acad Sci U S A. 2013; 110:2407–2412. [PubMed: 23345424]

Besson A, Dowdy SF, Roberts JM. CDK inhibitors: cell cycle regulators and beyond. Dev Cell. 2008; 14:159–169. [PubMed: 18267085]

Bhattacharjee S, Halane MK, Kim SH, Gassmann W. Pathogen effectors target Arabidopsis EDS1 and alter its interactions with immune regulators. Science. 2011; 334:1405–1408. [PubMed: 22158819]

Bonardi V, Tang S, Stallmann A, Roberts M, Cherkis K, Dangl JL. Expanded functions for a family of plant intracellular immune receptors beyond specific recognition of pathogen effectors. Proc Natl Acad Sci U S A. 2011; 108:16463–16468. [PubMed: 21911370]

Bowling SA, Clarke JD, Liu YD, Klessig DF, Dong XN. The cpr5 mutant of Arabidopsis expresses both NPR1-dependent and NPR1-independent resistance. Plant Cell. 1997; 9:1573–1584. [PubMed: 9338960]

Chandran D, Rickert J, Huang Y, Steinwand MA, Marr SK, Wildermuth MC. Atypical E2F transcriptional repressor DEL1 acts at the intersection of plant growth and immunity by controlling the hormone salicylic acid. Cell Host Microbe. 2014; 15:506–513. [PubMed: 24721578]

Chen H, Zou Y, Shang Y, Lin H, Wang Y, Cai R, Tang X, Zhou JM. Firefly luciferase complementation imaging assay for protein-protein interactions in plants. Plant Physiol. 2008; 146:368–376. [PubMed: 18065554]

Cheng YT, Germain H, Wiermer M, Bi D, Xu F, Garcia AV, Wirthmueller L, Despres C, Parker JE, Zhang Y, et al. Nuclear pore complex component MOS7/Nup88 is required for innate immunity and nuclear accumulation of defense regulators in Arabidopsis. Plant Cell. 2009; 21:2503–2516. [PubMed: 19700630]

Clarke JD, Aarts N, Feys BJ, Dong XN, Parker JE. Constitutive disease resistance requires EDS1 in the Arabidopsis mutants cpr1 and cpr6 and is partially EDS1-dependent in cpr5. Plant J. 2001; 26:409–420. [PubMed: 11439128]

Clarke JD, Volko SM, Ledford H, Ausubel FM, Dong XN. Roles of salicylic acid, jasmonic acid, and ethylene in cpr-induced resistance in arabidopsis. Plant Cell. 2000; 12:2175–2190. [PubMed: 11090217]

Coll NS, Vercammen D, Smidler A, Clover C, Van Breusegem F, Dangl JL, Epple P. Arabidopsis Type I Metacaspases Control Cell Death. Science. 2010; 330:1393–1397. [PubMed: 21097903]

De Veylder L, Beeckman T, Beemster GT, Krols L, Terras F, Landrieu I, van der Schueren E, Maes S, Naudts M, Inze D. Functional analysis of cyclin-dependent kinase inhibitors of Arabidopsis. Plant Cell. 2001; 13:1653–1668. [PubMed: 11449057]

De Veylder L, Beeckman T, Inze D. The ins and outs of the plant cell cycle. Nat Rev Mol Cell Biol. 2007; 8:655–665. [PubMed: 17643126]

Durrant WE, Dong XN. Systemic acquired resistance. Annu Rev Phytopathol. 2004; 42:185–209. [PubMed: 15283665]

Feys BJ, Moisan LJ, Newman MA, Parker JE. Direct interaction between the Arabidopsis disease resistance signaling proteins, EDS1 and PAD4. EMBO J. 2001; 20:5400–5411. [PubMed: 11574472]

Fu ZQ, Yan S, Saleh A, Wang W, Ruble J, Oka N, Mohan R, Spoel SH, Tada Y, Zheng N, et al. NPR3 and NPR4 are receptors for the immune signal salicylic acid in plants. Nature. 2012; 486:228–232. [PubMed: 22699612]

Harashima H, Dissmeyer N, Schnittger A. Cell cycle control across the eukaryotic kingdom. Trends Cell Biol. 2013; 23:345–356. [PubMed: 23566594]

Harbour JW, Dean DC. The Rb/E2F pathway: expanding roles and emerging paradigms. Genes Dev. 2000; 14:2393–2409. [PubMed: 11018009]

Heidrich K, Wirthmueller L, Tasset C, Pouzet C, Deslandes L, Parker JE. Arabidopsis EDS1 Connects Pathogen Effector Recognition to Cell Compartment-Specific Immune Responses. Science. 2011; 334:1401–1404. [PubMed: 22158818]

Jones JD, Dangl JL. The plant immune system. Nature. 2006; 444:323–329. [PubMed: 17108957]

Kirik V, Bouyer D, Schobinger U, Bechtold N, Herzog M, Bonneville JM, Hulskamp M. CPR5 is involved in cell proliferation and cell death control and encodes a novel trans membrane protein. Curr Biol. 2001; 11:1891–1895. [PubMed: 11728314]

Mackey D, Holt BF 3rd, Wiig A, Dangl JL. RIN4 interacts with Pseudomonas syringae type III effector molecules and is required for RPM1-mediated resistance in Arabidopsis. Cell. 2002; 108:743–754. [PubMed: 11955429]

Magyar Z, Horvath B, Khan S, Mohammed B, Henriques R, De Veylder L, Bako L, Scheres B, Bogre L. Arabidopsis E2FA stimulates proliferation and endocycle separately through RBR-bound and RBR-free complexes. EMBO J. 2012; 31:1480–1493. [PubMed: 22307083]

Pajerowska-Mukhtar KM, Wang W, Tada Y, Oka N, Tucker CL, Fonseca JP, Dong XN. The HSF-like transcription factor TBF1 is a major molecular switch for plant growth-to-defense transition. Curr Biol. 2012; 22:103–112. [PubMed: 22244999]

Parker JE, Holub EB, Frost LN, Falk A, Gunn ND, Daniels MJ. Characterization of eds1, a mutation in Arabidopsis suppressing resistance to Peronospora parasitica specified by several different RPP genes. Plant Cell. 1996; 8:2033–2046. [PubMed: 8953768]

Polager S, Ginsberg D. E2F - at the crossroads of life and death. Trends Cell Biol. 2008; 18:528–535. [PubMed: 18805009]

Polager S, Ginsberg D. p53 and E2f: partners in life and death. Nat Rev Cancer. 2009; 9:738–748. [PubMed: 19776743]

Qi D, DeYoung BJ, Innes RW. Structure-Function Analysis of the Coiled-Coil and Leucine-Rich Repeat Domains of the RPS5 Disease Resistance Protein. Plant Physiol. 2012; 158:1819–1832. [PubMed: 22331412]

Rusterucci C, Aviv DH, Holt BF 3rd, Dangl JL, Parker JE. The disease resistance signaling components EDS1 and PAD4 are essential regulators of the cell death pathway controlled by LSD1 in Arabidopsis. Plant Cell. 2001; 13:2211–2224. [PubMed: 11595797]

Schnittger A, Weinl C, Bouyer D, Schobinger U, Hulskamp M. Misexpression of the cyclin-dependent kinase inhibitor ICK1/KRP1 in single-celled Arabidopsis trichomes reduces endoreduplication and cell size and induces cell death. Plant Cell. 2003; 15:303–315. [PubMed: 12566574]

Sherr CJ, Roberts JM. CDK inhibitors: positive and negative regulators of G1-phase progression. Genes Dev. 1999; 13:1501–1512. [PubMed: 10385618]

Starostina NG, Kipreos ET. Multiple degradation pathways regulate versatile CIP/KIP CDK inhibitors. Trends Cell Biol. 2012; 22:33–41. [PubMed: 22154077]

Ting JPY, Willingham SB, Bergstralh DT. NLRs at the intersection of cell death and immunity. Nat Rev Immunol. 2008; 8:372–379. [PubMed: 18362948]

Vandepoele K, Vlieghe K, Florquin K, Hennig L, Beemster GT, Gruissem W, Van de Peer Y, Inze D, De Veylder L. Genome-wide identification of potential plant E2F target genes. Plant Physiol. 2005; 139:316–328. [PubMed: 16126853]

Verkest A, Manes CL, Vercruysse S, Maes S, Van Der Schueren E, Beeckman T, Genschik P, Kuiper M, Inze D, De Veylder L. The cyclin-dependent kinase inhibitor KRP2 controls the onset of the endoreduplication cycle during Arabidopsis leaf development through inhibition of mitotic CDKA;1 kinase complexes. Plant Cell. 2005; 17:1723–1736. [PubMed: 15863515]

Vlot AC, Dempsey DA, Klessig DF. Salicylic Acid, a multifaceted hormone to combat disease. Annu Rev Phytopathol. 2009; 47:177–206. [PubMed: 19400653]

Walker JD, Oppenheimer DG, Concienne J, Larkin JC. SIAMESE, a gene controlling the endoreduplication cell cycle in Arabidopsis thaliana trichomes. Development. 2000; 127:3931–3940. [PubMed: 10952891]

Wang H, Fowke LC, Crosby WL. A plant cyclin-dependent kinase inhibitor gene. Nature. 1997; 386:451–452. [PubMed: 9087400]

Wang S, Durrant WE, Song J, Spivey NW, Dong XN. Arabidopsis BRCA2 and RAD51 proteins are specifically involved in defense gene transcription during plant immune responses. Proc Natl Acad Sci U S A. 2010; 107:22716–22721. [PubMed: 21149701]

Wang W, Barnaby JY, Tada Y, Li H, Tor M, Caldelari D, Lee DU, Fu XD, Dong XN. Timing of plant immune responses by a central circadian regulator. Nature. 2011; 470:110–114. [PubMed: 21293378]

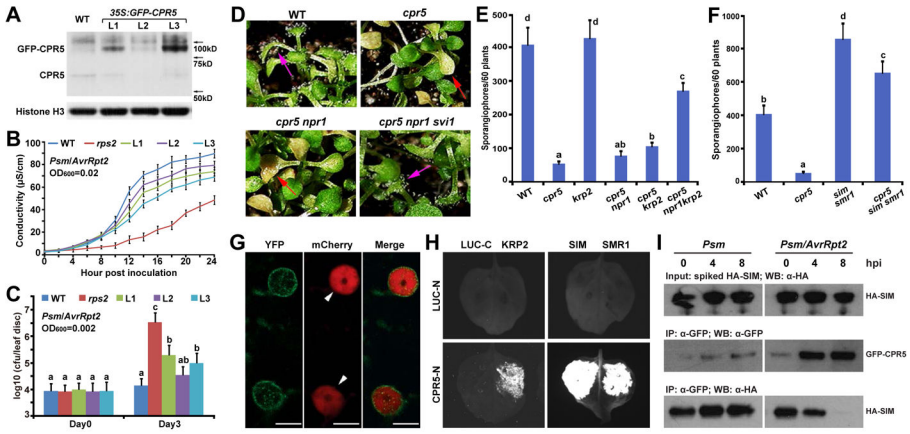

Figure 1. The Nuclear Envelope Protein CPR5 Negatively Regulates Effector-Triggered PCD and Resistance through Interactions with CKIs

(A) Nuclear proteins were purified from 2-week-old WT and three independent *35S:GFP-CPR5* transgenic plants in the *cpr5-1* mutant background (L1, L2 and L3). The western blot was probed with α-CPR5 and α-histone H3.

(B) Three-week-old WT, *rps2* and *35S:GFP-CPR5* transgenic plants were inoculated with *Psm* ES4326/*AvrRpt2* (OD_{600} = 0.02). Leaf discs were harvested 30 minutes after inoculation and ion leakage was measured every 2 hours using the conductivity assay. Error bars represent SEs. Experiments were carried out two times with similar results.

(C) WT, *rps2* and *35S:GFP-CPR5* transgenic plants were inoculated with *Pseudomonas syringae* (*Psm*) ES4326/*AvrRpt2* (OD_{600} = 0.002). Bacterial growth (cfu, colony forming unit) was measured right after inoculation (Day 0) and 3 days later (Day 3). Error bars represent 95% confidence intervals (n = 8). Experiments were conducted three times with similar results.

(D) *Arabidopsis* seedlings (7 to 10-day-old) were inoculated with *Hpa* Noco2 spores (5×10^4 spores/ml). *Hpa* sporangiophores (pink arrow) and *cpr5*-mediated early senescence (red arrow) were visualized 7 days later.

(E) and (F) *Arabidopsis* seedlings were inoculated with *Hpa* Noco2 spores (5×10^4 spores/ml). After 7 days, the sporangiophores were counted after trypan blue staining. Error bars represent SEs. Experiments were conducted three times with similar results.

(G) BiFC assay was carried out in *Nicotiana benthamiana* leaves. The N- and C-terminus of yellow fluorescent protein (YFP) were fused to SIM (SIM-nYFP) and full-length CPR5 (cYFP-CPR5), respectively. The free mCherry served as a nuclear marker.

(H) Split luciferase assay was performed in *N. benthamiana* leaves. The N-terminus of luciferase (LUC-N) was fused to the C-terminus of CPR5 (N-terminal 339 amino acids), and the C-terminal half of luciferase (LUC-C) was fused to the N-terminus of KRP2, SIM or SMR1.

(I) Leaves of *35S:GFP-CPR5* transgenic plants (four-week-old) were infiltrated with *Psm* ES4324 or *Psm* ES4326/*AvrRpt2* at OD_{600} = 0.02. Total proteins were extracted at indicated hour past infiltration (hpi) and co-immunoprecipitated (co-IP) with wheat germ- synthesized HA-SIM. The input HA-SIM protein was taken at end of the co-IP incubation and detected using western blot with α-HA. The binding of HA-SIM to GFP-CPR5 was detected by western blot using the antibodies α-GFP and α-HA.

See also Figure S1 and Tables S1 and S2.

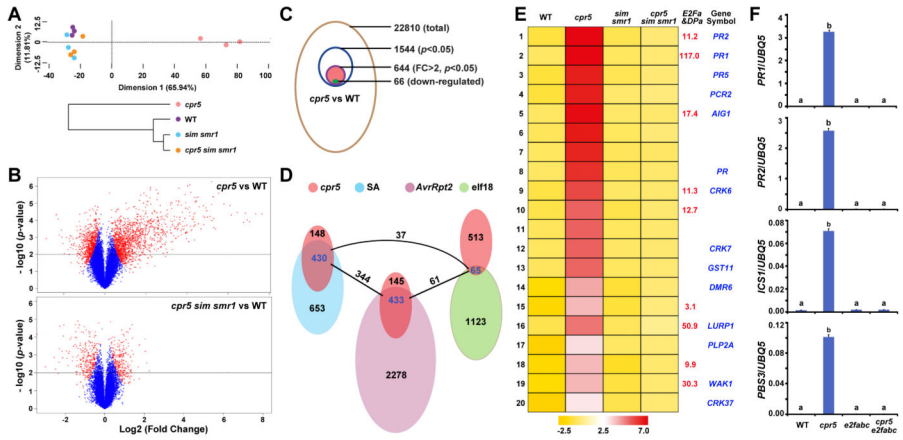

Figure 2. CPR5 Regulates ETI-Specific Defense Gene Expression through SIM/SMR1 and E2F

(A) Principal component analysis of the microarray data and hierarchical clustering of the averaged genomic expression pattern. Genotypes with replicates were color labeled. The microarray experiments were conducted using 10-day-old plants in three biological replicates.

(B) Volcano plots illustrating differentially expressed genes (*p*-value <0.01) with permutation (n=1000) in *cpr5* and *cpr5 sim smr1* compared to WT. James-Stein shrinkage estimates of the error variance were used.

(C) Summary of differential gene expression in the *cpr5* mutant comparing to WT. Student's *t*-test is used and *p*-values are computed asymptotically and subject to Benjamini-Hochberg adjustment. FC, fold change.

(D) Comparative analysis of *cpr5* microarray data with defense-related data sets (GSE34047, GSE58954). Lists of upregulated genes were generated using *t*-test with *p*-value <0.05, FC>2.

(E) The top 20 *cpr5*-induced genes (*p*-value<0.05), shown in the heatmap, include 14 designated as defense-related (named in blue) and 9 E2Fa/DPa-target genes (Vandepoele et al., 2005) (reported fold induction in E2Fa/DPa-overexpressing plants is shown in red). *PATHOGENESIS-RELATED 1/2/5* (*PR1/2/5*), *PLANT CADMIUM RESISTANCE 2* (*PCR2*), *AVRRPT2-INDUCED GENE 1* (*AIG1*), *CYSTEINE-RICH RLK 6/7/37* (*CRK6/7/37*), *GLUTATHIONE S-TRANSFERASE 11* (*GST11*), *DOWNY MILDEW RESISTANT 6* (*DMR6*), *LATE UPREGULATED IN RESPONSE TO HYALOPERONOSPORA PARASITICA 1* (*LURP1*), *PHOSPHOLIPASE A 2A* (*PLP2A*), *CELL WALL-ASSOCIATED KINASE 1* (*WAK1*).

(F) Quantitative RT-PCR was performed on *PR1*, *PR2*, *ICS1* and *PBS3* in 10-day-old seedlings. *UBQ5* was used as an internal control. Error bars represent SEs. Experiments were conducted in triplicate.

See also Figure S2 and Tables S3 and S4.

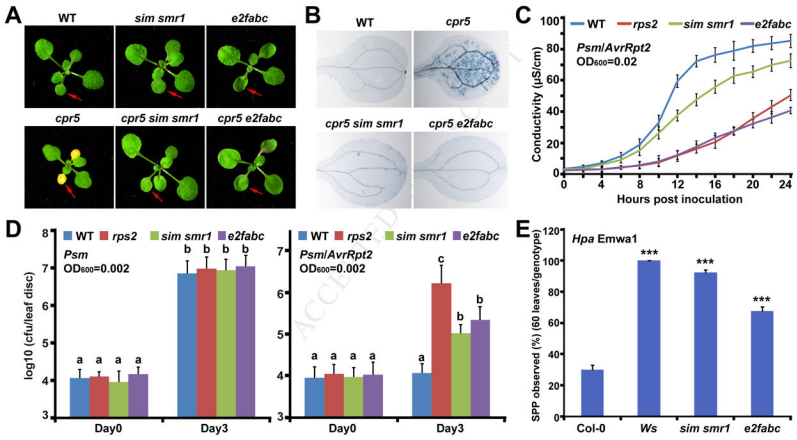

Figure 3. SIM/SMR1 and E2F Are Required for *cpr5*-Mediated and Effector-Triggered PCD and Immunity

(A) Two-week-old plants were examined and photographed for early senescence of cotyledons (arrow heads).

(B) Two-week-old cotyledons were stained using trypan blue for cells that have undergone PCD.

(C) Four-week-old plants were infected with *Psm* ES4326/*AvrRpt2* (OD_{600} = 0.02). Leaf discs were harvested 30 minutes after inoculation, and ion leakage was measured every 2 hours. Error bars represent SEs. Experiments were carried out three times with similar results.

(D) Four-week-old plants were inoculated with *Psm* ES4326 (left panel) or *Psm* ES4326/*AvrRpt2* (right panel) (OD_{600} = 0.002; a high dosage normally used for observing ETI). Bacterial growth (cfu, colony forming unit) was measured right after inoculation (Day 0) and 3 days later (Day 3). Error bars represent 95% confidence intervals (n = 8). Experiments were conducted three times with similar results.

(E) Seven-day-old seedlings were inoculated with a suspension of asexual spores (5×10^5 spores per ml) of *Hpa* Emwa1. The RPP4-deficient Ws accession was used as a negative control. Plants were collected 7 days post inoculation (dpi), stained with trypan blue, and scored for the presence of sporangiophores (SPP). Error bars represent SD, *** *p*-value <0.001 compared to WT by binomial distribution. Experiment was repeated three times with similar results.

See also Figure S3.

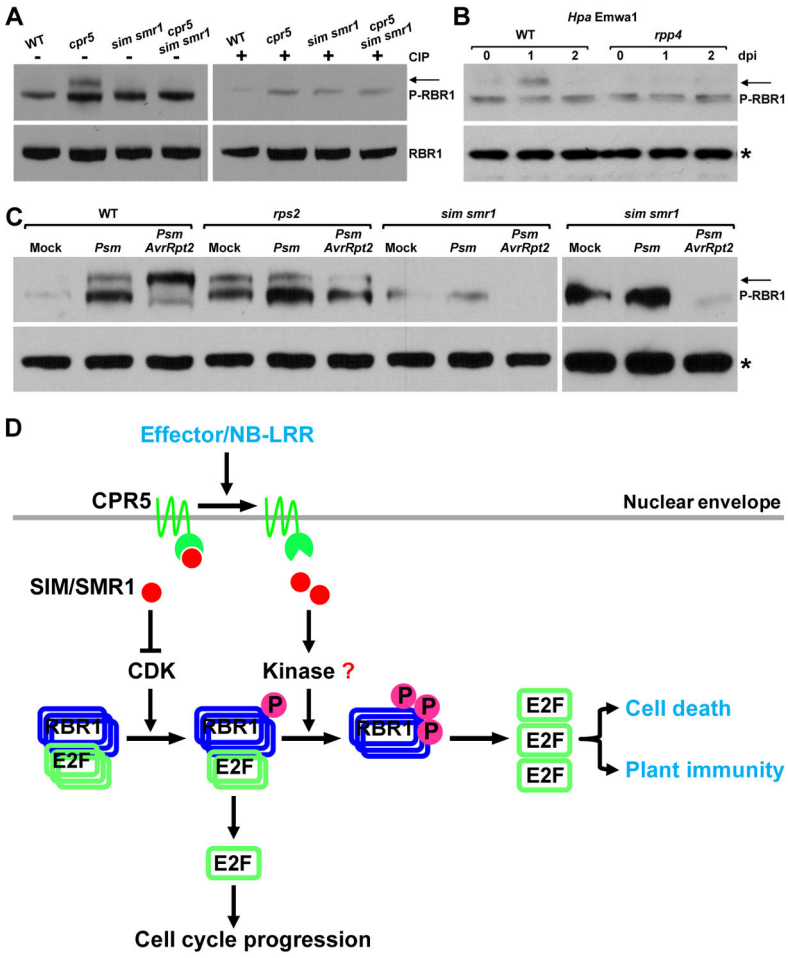

Figure 4. SIM and SMR1 Confer Plant PCD and Immunity through Hyperphosphorylation of RBR1

(A) Western blot analysis was performed on protein extracts from 10-day-old plants. α-P-RB and α-RBR1 were used to detect phosphorylated and total *At*RBR1, respectively. The hyperphosphorylated *At*RBR1 in *cpr5* is indicated by an arrow. The same set of samples was treated with CIP (+) to dephosphorylate the protein.

(B) Seven-day-old seedlings were inoculated with *Hpa* Emwa1. Samples were taken at 0, 1 and 2 days post inoculation (dpi). α-P-RB was used to detect phosphorylated *At*RBR1. The hyperphosphorylated *At*RBR1 is marked by an arrow. * indicates a nonspecific band used as a loading control.

(C) Three-week-old plants were inoculated with 10 mM $MgCl_2$ (Mock), *Psm* ES4326 (*Psm*; OD_{600} = 0.02) and *Psm* ES4326/*AvrRpt2* (*Psm AvrRpt2*; OD_{600} = 0.02). Protein extracts were made 12 hours later and analyzed by western blotting using α-P-RB. To better visualize the signals of the last three lanes (left panel), a longer exposure of the film is also shown (right panel). The hyperphosphorylated *At*RBR1 is marked by an arrow. * indicates a nonspecific band used as a loading control.

(D) Proposed downstream signaling events in effector-triggered PCD and immunity. Under normal conditions, SIM and SMR1 serve as CDK inhibitors in regulation of cell cycle progression. Recognition of a pathogen effector by the cognate NB-LRR triggers

dissociation of SIM and SMR1 from the nuclear envelope protein CPR5. Consequently, SIM and SMR1 acquire a novel activity of facilitating RB hyperphosphoryation through an unknown kinase (?), resulting in E2F over-activation and effector-triggered PCD and disease resistance.

See also Figure S4.